FLORE
Repository istituzionale dell'Università degli Studi di Firenze

Self-Assembly of Manganese(II)–Phytate Coordination Polymers: Synthesis, Crystal Structure, and Physicochemical Properties

Questa è la Versione finale referata (Post print/Accepted manuscript) della seguente pubblicazione:

Original Citation:

Self-Assembly of Manganese(II)–Phytate Coordination Polymers: Synthesis, Crystal Structure, and Physicochemical Properties / Quiñone, D.; Veiga, N.; Torres, J.; Bazzicalupi, C.; Bianchi, A.; Kremer, C.. - In: CHEMPLUSCHEM. - ISSN 2192-6506. - STAMPA. - 82:(2017), pp. 721-731. [10.1002/cplu.201700027]

Availability:

This version is available at: 2158/1080781 since: 2018-03-09T11:50:32Z

Published version:

DOI: 10.1002/cplu.201700027

Terms of use:

Open Access

La pubblicazione è resa disponibile sotto le norme e i termini della licenza di deposito, secondo quanto stabilito dalla Policy per l'accesso aperto dell'Università degli Studi di Firenze (https://www.sba.unifi.it/upload/policy-oa-2016-1.pdf)

Publisher copyright claim:

(Article begins on next page)

23 April 2024

A GENUINELY MULTIDISCIPLINARY JOURNAL

CHEMPLUSCHEM

CENTERING ON CHEMISTRY

Accepted Article

Title: Self-Assembly of Mn(II)-Phytate Coordination Polymers: Synthesis, Crystal Structure and Physicochemical Properties

Authors: Antonio Bianchi, Delfina Quiñone, Nicolás Veiga, Julia Torres, Carla Bazzicalupi, and Carlos Kremer

This manuscript has been accepted after peer review and appears as an Accepted Article online prior to editing, proofing, and formal publication of the final Version of Record (VoR). This work is currently citable by using the Digital Object Identifier (DOI) given below. The VoR will be published online in Early View as soon as possible and may be different to this Accepted Article as a result of editing. Readers should obtain the VoR from the journal website shown below when it is published to ensure accuracy of information. The authors are responsible for the content of this Accepted Article.

To be cited as: *ChemPlusChem* 10.1002/cplu.201700027

Link to VoR: http://dx.doi.org/10.1002/cplu.201700027

A Journal of

ChemPubSoc Europe

WILEY-VCH

www.chempluschem.org

Self-Assembly of Mn(II)-Phytate Coordination Polymers: Synthesis, Crystal Structure and Physicochemical Properties

Delfina Quiñone,[a] Nicolás Veiga,[a] Julia Torres,[a] Carla Bazzicalupi,[b] Antonio Bianchi,*[b] and Carlos Kremer*[a]

Abstract: *myo*-inositol phosphates are an important group of biomolecules present in all eukaryotic cells. The most abundant member of this family in nature is InsP_6 (phytate, L^{12-} in its fully deprotonated form). Phytate interacts strongly with inorganic and organic cations, and this interaction is essential for determining the possible functions of this biomolecule. We present here the chemical, thermodynamic and structural characterization of phytate-Mn(II) species in a contribution to understand how the interaction of both components modulates their biological roles and their bioavailability. Polynuclear complexes $Mn_5(H_2L)\cdot16H_2O$ (**1**) and $(H_2terpy)_2[Mn(H_6L)(terpy)(H_2O)]\cdot17H_2O$ (terpy = terpyridine) (**2**) were prepared and characterized by different techniques. The isolation of **1**, and the determination of its solubility, together with potentiometric titrations of the Mn(II)-phytate system allowed the full description of this binary systems. The preparation and crystal structure of **2** shows a novel coordination mode of phytate, the formation of infinite polymeric chains through equatorial phosphate groups.

Introduction

Among the first row transition metals, the element manganese is second only to iron in terms of its terrestrial abundance.[1] Given the relative abundance and accessibility of manganese in the biosphere, the versatility of its coordination chemistry, and its broad range of oxidation states, it is not surprising that diverse plant and animal life forms have evolved with a requirement for this metal ion as an essential trace element.[2] The concentration of Mn(II) is close to 10^{-7} M almost inside or outside cells;[3] its concentration reaches 0.11 µM in human plasma,[4] and 0.25 - 0.7 µM in rat hepatocytes.[5]

Manganese is most commonly associated with its role as a catalytic and/or structural protein cofactor.[6] Nevertheless, the majority of the intracellular manganese is thought to be present as low molecular-weight Mn(II) complexes[7] that, among other functions, can act independently of proteins to either defend against[8] or promote[9] oxidative stress and disease.

In this context, it is widely accepted that the understanding of manganese speciation in cells is critical for deciphering the mechanisms by which cells appropriately handle this "essential toxin", and for addressing the role of manganese in human health and disease. Even though it has been recently reported that approximately 24 % of the intracellular chelatable manganese is present as complexes with polyphosphate ligands,[10] the chemical nature of those species remains unknown.

One polyphosphate anion that stands a chance to act as a low molecular-weight ligand for the chelatable intracellular manganese pool is phytate (InsP_6, L^{12-}, Figure 1). It is by far the most abundant inositol polyphosphate in eukaryotic cells, with a concentration in mammalian cells in the range 10-60 µM and up to 0.7 mM in slime moulds.[11] Phytate exhibits a strong interaction with any cation present in physiological media because it is highly charged (the predominant species are H_4L^{8-} and H_5L^{7-}).[12] In the cytosolic/nuclear compartment, InsP_6 is predicted to exist as the polymetallic complex $[Mg_5(H_2L)]$.[13] The solubility of this species limits the amount of protein-free InsP_6 under these intracellular conditions. The relevance of its interaction with Mn(II) cannot be ruled out. Phytate forms highly stable 1:1 complexes with Mn(II) in solution,[12, 14] and has been found precipitated with this metal ion as globoid crystals in grains.[15] The latter exemplifies a common trend in nature: the phytate anion is the major phosphorous component of plants and, in particular, cereal grains.[16] That being said, phytate has long been known as an antinutritional factor, since it can precipitate several minerals from the diet in the gut. Thus, the interest in studying the phytate-Mn(II) interaction is also due to the fact that the complexation and precipitation processes that phytate undergoes in the presence of multivalent cations modulate manganese bioavailability. Certainly, it has been proved that the presence of phytate in soy decreases the manganese intestinal absorption.[17]

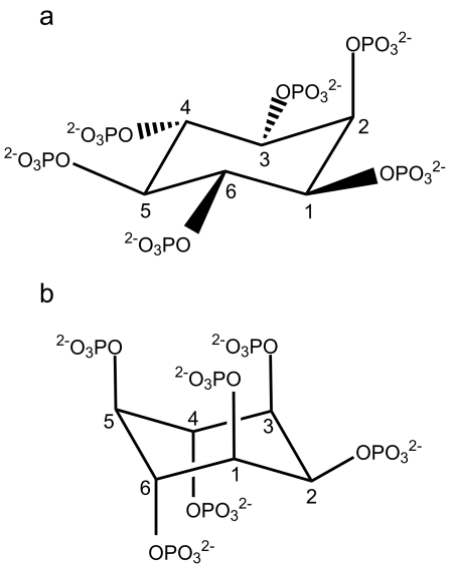

Figure 1. Structure of InsP_6 (L^{12-}) for both conformations: (a) 1 axial-5 equatorial (1a5e) and (b) 5 axial-1 equatorial (5a1e).

[a] D. Quiñone, Dr. N. Veiga, Prof. J. Torres, Prof. C. Kremer
Departamento Estrella Campos
Facultad de Química, Universidad de la República
General Flores 2124, Montevideo, Uruguay
E-mail: ckremer@fq.edu.uy
[b] Prof. C. Bazzicalupi, Prof. Antonio Bianchi
Dipartimento di Chimica "Ugo Schiff"
Universitá degli Studi di Firenze
Via della Lastruccia, 3, 50019 Sesto Fiorentino, Italy.
E-mail: antonio.bianchi@unifi.it

Supporting information for this article is given via a link at the end of the document.

Accepted Manuscript

This article is protected by copyright. All rights reserved.

In the light of the above, the chemical, thermodynamic and structural characterization of phytate-Mn(II) species is essential to understand how the interaction of both components modulates their biological roles and their bioavailability. Even though highly stable [Mn(H_xL)] species, with x = 0 – 5, were detected in solution,[12, 14, 18] the chemical nature and solubility of the sparingly soluble phytate-Mn(II) solid phases were poorly addressed. Indeed, there is only one report that dealt with this matter,[19] but no solubility product was determined. Without this parameter, a complete thermodynamic picture of the chemical behavior of manganese in the presence of different amounts of phytate cannot be given.

Until now, the use of X-ray diffraction techniques to obtain further structural data of metal-phytate solids has been restricted by the amorphous characteristic of these phases. In the past two years, our group made a breakthrough in this field, reporting three new structures of Cu(II)-InsP_6 complexes determined by X-ray diffraction.[20] These compounds were obtained by the use of an aromatic rigid amine (terpyridine, phenanthroline), which acts as an auxiliary ligand, satisfying some of the metal coordination sites and promoting the crystallization of the solid phases.

Following the same strategy, in this work we report the synthesis and chemical characterization of the Mn(II)-phytate solid phase. Then, the solubility product of this phase was determined under simulated physiological conditions (0.15 M $NaClO_4$, 37.0 °C). With this data, we were able to furnish a complete picture of the chemical behavior of the system under different conditions. In order to get structural information on the Mn(II)-phytate interaction, terpyridine (terpy) was added as a co-ligand, and the first crystalline structure of a Mn(II)-phytate complex, $(H_2terpy)_2[Mn(H_6L)(terpy)(H_2O)]\cdot 17H_2O$, was elucidated by X-ray diffraction. This information, coupled with potentiometric and computational data of the soluble Mn(II)-phytate-terpy species, allowed us to shed light on the multifaceted coordination ability of InsP_6 in the presence of manganese(II).

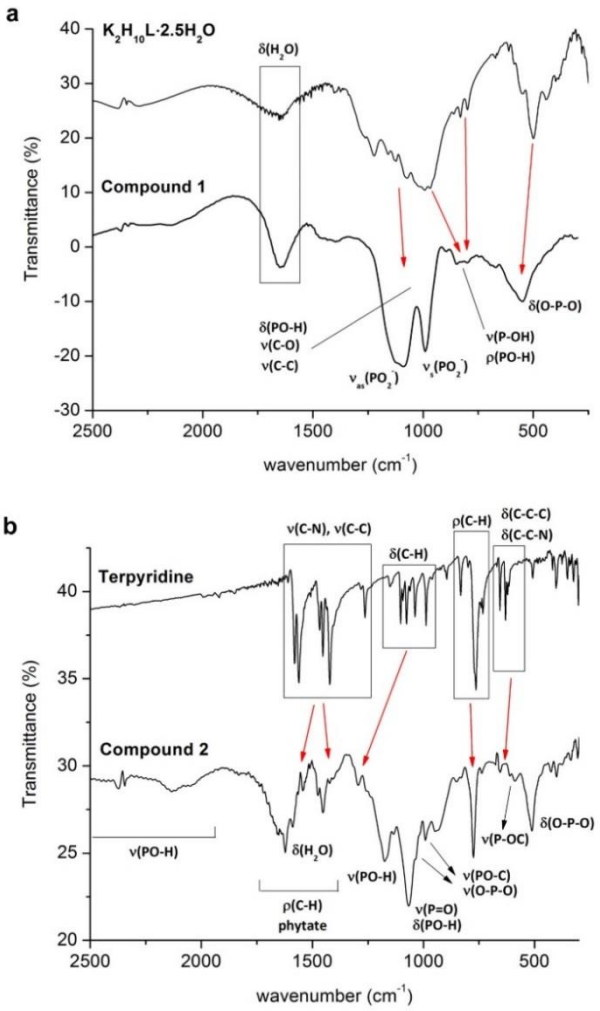

Figure 2. Infrared spectra of compounds **1** (a) and **2** (b). The vibrational spectra of the dipotassium salt and terpyridine are shown for comparison. Complete range spectra are shown in Figure S2.

Results and Discussion

Characterization of manganese(II) phytate

Stoichiometry

The manganese(II) phytate synthesized in this work was found to have the same stoichiometry already reported for the Ca, Sr and Ba phytates: $Mn_5(H_2L)\cdot 16H_2O$ (**1**).[13, 21] The same 5:1 metal-to-ligand ratio was also reported for other phytates,[12, 22] which suggests similar structures for those InsP_6 solids. However, the ligand protonation state (H_2L^{10-}) is only compatible with previous reports on magnesium, calcium[12-13, 22f-h], strontium, barium[21] and cobalt(II)[22e] phytates.

The unique manganese(II) phytate reported to date was synthesized at pH 7 – 8 in a methanol:water mixture (20:1, v:v), and yielded the formula $Na_3Mn_5L(OH)\cdot 9H_2O$.[19] This is a peculiar result, since at neutral pH the phytate anion is protonated to a great extent (H_4L^{8-} and H_5L^{7-})[12] and the OH^- concentration is certainly low. In this work, however, we prepared the solid phase **1** from an aqueous solution of phytate, in order to adequately represent the InsP_6 precipitation process that may occur in the presence of Mn(II) in environmental or biological aqueous media

Infrared spectroscopy and thermal analysis

The infrared spectrum of **1** is shown in Figure 2a. In order to analyze the normal modes associated with the most important IR bands and their change upon complexation and deprotonation of the ligand, we began by performing a detailed assignation of the spectral infrared profile of $K_2H_{10}L\cdot 2.5H_2O$. To do this, we conducted gas phase Hartree-Fock calculations on the totally protonated species of phytate, $H_{12}L$, as a model of the $H_{10}L^{2-}$ anion present in the dipotassium salt. Further details on the assignment of the $K_2H_{10}L\cdot 2.5H_2O$ infrared bands are presented in the ESI (Figure S1).

Between 3700 and 2500 cm^{-1}, the $K_2H_{10}L\cdot 2.5H_2O$ salt shows a medium intense broad band ascribed to the stretching of O–H bonds, in line with reported data for $Ca(H_2PO_4)_2\cdot H_2O$.[23] The intensity of this band increases substantially in **1**, due to the presence of a much larger amount of crystallized solvent.

Accepted Manuscript

This article is protected by copyright. All rights reserved.

Table 1. Determination of K_{s0} for Mn(II) phytate (0.15 M $NaClO_4$ at 37.0 °C).

Entry	$[Mn(II)]_{tot}$ (mM)[a]	$[InsP_6]_{tot}$ (mM)[b]	$[H^+]_{tot}$ (mM)[c]	$[Mn(II)]_{free}$ (mM)[c]	$[H_2L^{10-}]_{free}$ (M)[d]	log K_{s0}
1	3.32	0.66	6.05	2.67	2.5×10^{-28}	–40.5
2	5.11	1.02	10.5	4.15	1.3×10^{-29}	–40.8
3	11.2	2.24	18.6	9.04	7.4×10^{-30}	–39.4
4	17.6	3.52	27.8	14.2	2.8×10^{-30}	–38.8

[a] Total concentration of Mn determined in the saturated solution. [b] $[InsP_6]_{tot}$ corresponds to 1/5 the amount of Mn(II). [c] $[H^+]_{tot}$ is calculated as $[H^+]$ added plus 2 times the total amount of $InsP_6$, according to the stoichiometry of the solid phytate. [d] Free equilibrium concentrations calculated using HySS software.[24]

Quantification of water content by thermogravimetric analysis showed that the sixteen water molecules in **1** were lost across a wide temperature range, namely between 30 and 200 °C (Figure S3). This is consistent with the presence of a set of weakly to strongly bonded water molecules, which according to the variation of the first derivative of the curve (not shown) are lost in two steps: from 30 to 80 °C (step 1) and from 80 to 200 °C (step 2). The first step corresponds to the release of *ca.* 12 water molecules (19 % weight loss), which are the weakest bound. The rest of the water content (4 molecules, 5.7 % weight loss) was lost at higher temperatures in the second step, and possibly represents those H_2O molecules linked to the metal centers. This result suggests that less than one water molecule is probably coordinated to each Mn(II) ion in **1**.

Just below 3000 cm^{-1}, the ν(C–H) normal modes of the inositol ring appears superimposed to the ν(O–H) broad and intense band of **1**. This is expected to occur for P-O-R compounds in the range 3030 – 2800 cm^{-1}.[25] The band at about 1655 cm^{-1} is not predicted among the computational results for $H_{12}L$ (Figure S1). It can be assigned to the bending of the H–O–H bonds of hydration water molecules,[23] and its fine structure can be accounted for by the presence of the infrared overtones of δ(PO–H) and ρ(PO–H) normal modes.[25]

The intense and broad band observed between 1400 and 700 cm^{-1} for $K_2H_{10}L{\cdot}2.5H_2O$ is associated with several normal modes of the phosphate groups (Figure S1). This band is split into three peaks upon complexation and deprotonation to form **1**. The first two, at around 1090 and 991 cm^{-1}, are assigned to the asymmetric and symmetric stretching of the PO_2^- groups. In fact, this two bands have been already reported for pyridoxal phosphate.[26] The third band appears in the region 849 – 791 cm^{-1}, and can be associated with ν(P–OH) and ρ(PO–H) vibrations, in agreement with evidence found for some copper complexes.[27] Finally, the peak at 546 cm^{-1} in **1** is attributed to the δ(O–P–O) normal mode, and is observed at higher wavenumbers than the same band in $K_2H_{10}L{\cdot}2.5H_2O$. The splitting and shifting of the bands related to the phosphate vibrations is a symptomatic of a direct and bidentate M-O-P coordination of the metal ion.[19, 28]

Solubility product

Following the same procedure applied for other bivalent phytates,[13, 21] we measured the solubility of the manganese(II) phytate. From a thermodynamic viewpoint, the solubility of **1** can be characterized by its solubility product constant $K_{s0} = [Mn^{2+}]^5[H_2L^{10-}]$. Determination of the K_{s0} value requires measuring sets of values for the concentrations of Mn^{2+} and H_2L^{10-} at equilibrium with the solid. These can be calculated from the straightforward analytical data by means of appropriate software such as HySS,[24] fed with the complete set of equilibrium constants for the protonation and complexation equilibria.[12] The results are shown in Table 1, and can be summarised in the solubility product:

$$Mn_5(H_2L){\cdot}16H_2O(s) \rightarrow 5\ Mn^{2+}(aq) + H_2L^{10-}(aq)\ \log K_{s0} = -39.9(9)$$

which is valid at 0.15 M $NaClO_4$ and 37.0 °C. This data can be compared with the logK_{s0} determined for the alkaline earth phytates under the same conditions: –32.93 (Mg), –39.3 (Ca), –35.6 (Sr), –38.3 (Ba).[13, 21] Taking into account their intrinsic solubilities (i.e. without considering the effects of the participation of $InsP_6$ in other equilibria in solution), the manganese(II) phytate is the less soluble of all these phytates, their solubility increasing according to Mn(II) < Ca < Ba < Sr < Mg.

A complete view of the manganese(II)-phytate interaction

A complete description of the behavior of $InsP_6$ in the presence of Mn(II) requires the thermodynamic characterization of all the equilibria involved. The logK_{s0} value determined for **1**, together with the protonation and Mn(II) complexation constants in solution previously reported by us under the same conditions,[12] were handled by the HySS program to calculate the species distribution shown in Figure 3a. Under equimolar conditions of phytate and Mn(II), 1:1 metal-to-ligand soluble complexes are present over the entire pH range, while the precipitation of **1** is predicted above pH = 7. Interestingly, with Mg(II) (with which $InsP_6$ is thought to be complexed in the cytosolic and nuclear compartments[13]) the phytate anion does not precipitate under the set of conditions chosen (Figure 3b). This low solubility behavior displayed by $InsP_6$ in the presence of Mn(II) is in line with the fact that phytate is commonly present in grains as solid globoid crystals containing this metal ion.[15]

Figures 4a and b summarize the behavior of $InsP_6$ in the presence of Mn(II) at physiological pH. For a fixed total manganese(II) concentration, the abundance of the solid phytate increases as the total $InsP_6$ concentration is raised, reaching a maximum near to the stoichiometric 5:1 Mn(II):$InsP_6$ ratio (Figure 4a). When $InsP_6$ concentration is increased beyond this point, the manganese(II) phytate is redissolved gradually, being replaced by the soluble 1:1 complexes (see Figure 4b). This "paradoxical' solubility behavior of $InsP_6$ was also reported for

Accepted Manuscript

This article is protected by copyright. All rights reserved.

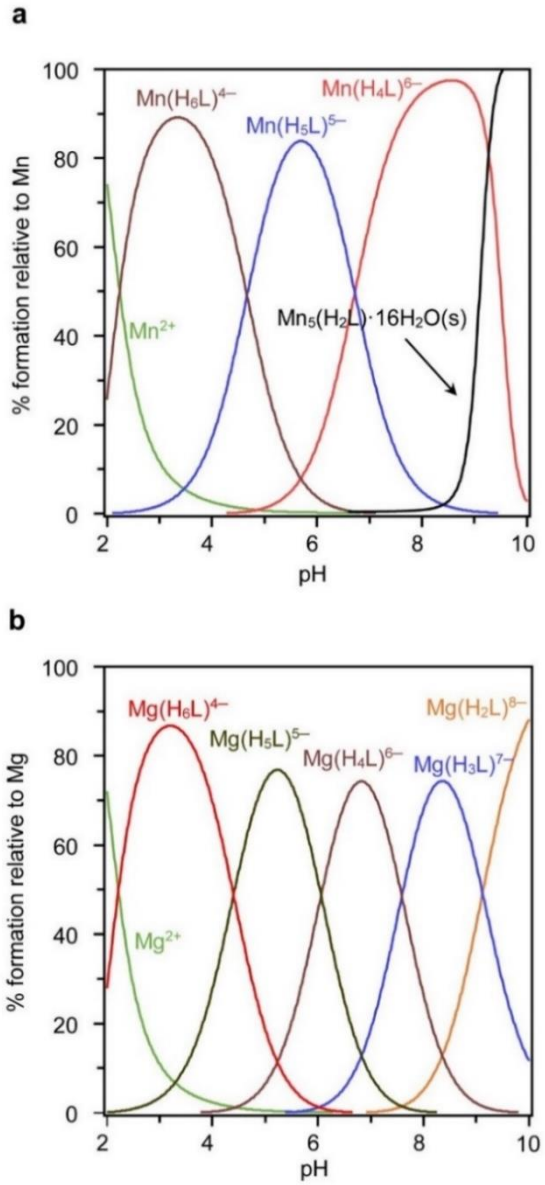

Figure 3. Chemical speciation of phytate in the presence of Mn(II) (a) or Mg (b)[12-13] as the pH varies. The diagrams are drawn for 1 mM total M(II), 1 mM total InsP_6, 37.0 °C and *I* = 0.15 M $NaClO_4$.

magnesium (Figures 4c and d), and can be rationalized on the basis of the excess InsP_6 acting, through the formation of the soluble 1:1 complexes, as a metal sequestering agent.[13]

The difference between the solubility profiles of Mn(II) and Mg phytates becomes evident when analyzing the behavior of the system in the low InsP_6 concentration range, where no 1:1 soluble species are predict to coexist (see the insets in Figures 4a and c). The manganese(II) concentration needed for a complete precipitation of the phytate anion is more than ten times lower than for magnesium. Even though this can be rationalized by the lower solubility product of manganese(II) phytate, this is not the only reason. Indeed, the behavior of InsP_6 in the presence of Mg^{2+} is slightly more complex due to the formation of the polynuclear complex $[Mg_5(H_2L)]$ (undetected for Mn(II)), which has a significant window of solubility under these conditions. Only when Mg and phytate concentrations are high enough, the polynuclear $[Mg_5(H_2L)]$ species starts to precipitate as $[Mg_5(H_2L)]\cdot 22H_2O(s)$ (see the inset in Figure 4c).[13]

Structural analysis of phytate coordination ability towards manganese(II)

First crystalline complex containing manganese(II) bound to phytate

The inclusion of terpyridine or phenanthroline (phen) as an auxiliary ligand allowed us recently to obtain the first three crystalline complexes of Cu(II) and InsP_6 ($[Cu_2(H_8L)(terpy)_2]\cdot 7.5H_2O$, $K[Cu_4(H_3L)(terpy)_4]\cdot 26H_2O$, and $[Cu_5(H_7L)_2(H_2O)_2(phen)_5]\cdot 23H_2O$), whose structures were solved by X-ray diffraction.[20] Along the same line, we present here the synthesis and characterization of the first crystalline complex between phytate and Mn(II), using terpyridine as a terminal ligand that prevents the scarcely soluble amorphous manganese(II) phytate to be formed in the system. When an equimolar solution of Mn(II), InsP_6 and terpy (pH = 2.6) was subjected to slow evaporation, yellow crystals of $(H_2terpy)_2[Mn(H_6L)(terpy)(H_2O)]\cdot 15H_2O$ (**2**) were obtained. Even though several experiments were carried out under a wide variety of conditions, we could only obtain a crystalline phase in an acid medium and in the absence of other competing anions, such as Cl^- or SO_4^{2-}. Compound **2** was characterized by elemental analysis, thermogravimetric measurements, and infrared spectroscopy. The assignment of the most important IR bands was made based on previous data reported for terpyridine,[29] and the abovementioned discussion for compound **1**. Additionally, we also made use of the detailed assignment already published for $[Cu_5(H_7L)_2(H_2O)_2(phen)_5]\cdot 23H_2O$,[20b] since its infrared spectral profile is similar to the one for compound **2** (Figure S4).

The infrared spectrum of **2** is depicted in Figure 2b. It shows a wide and strong absorption band in the range 3700 – 2000 cm^{-1}, ascribed to the O-H stretching modes. This band has two contributions: the coordinated and co-crystallized water molecules (3700-2800 cm^{-1}), and the protonated phosphate groups not involved in the net of H-bonds (2800 – 1800 cm^{-1}). The ν(C-H) normal modes of both ligands are superimposed to this band, being evidenced as less absorptive peaks in the range 3102 – 2845 cm^{-1}. Water bending vibration and phytate C–H deformation modes appear as a broad band centered at 1618 cm^{-1}. The superimposed, sharp medium intensity peaks observed between 1655 and 1420 cm^{-1} correspond to the C–C and C–N stretching and C–H bending modes of terpy. These vibrations are shifted in comparison to the same bands for the free ligand, which evidences metal complexation.[29]

In agreement with the infrared spectra of **1** (Figure 2a), the normal modes attributed to the phosphate groups are observed below 1300 cm^{-1} as broad and intense spectral bands. Strong peaks appear at 1175, 1067 and 993 cm^{-1}, being brought about by the stretching of the PO–H bonds engaged in H-bonds, the stretching of double P=O and single P–O and PO–C bonds, and

Accepted Manuscript

This article is protected by copyright. All rights reserved.

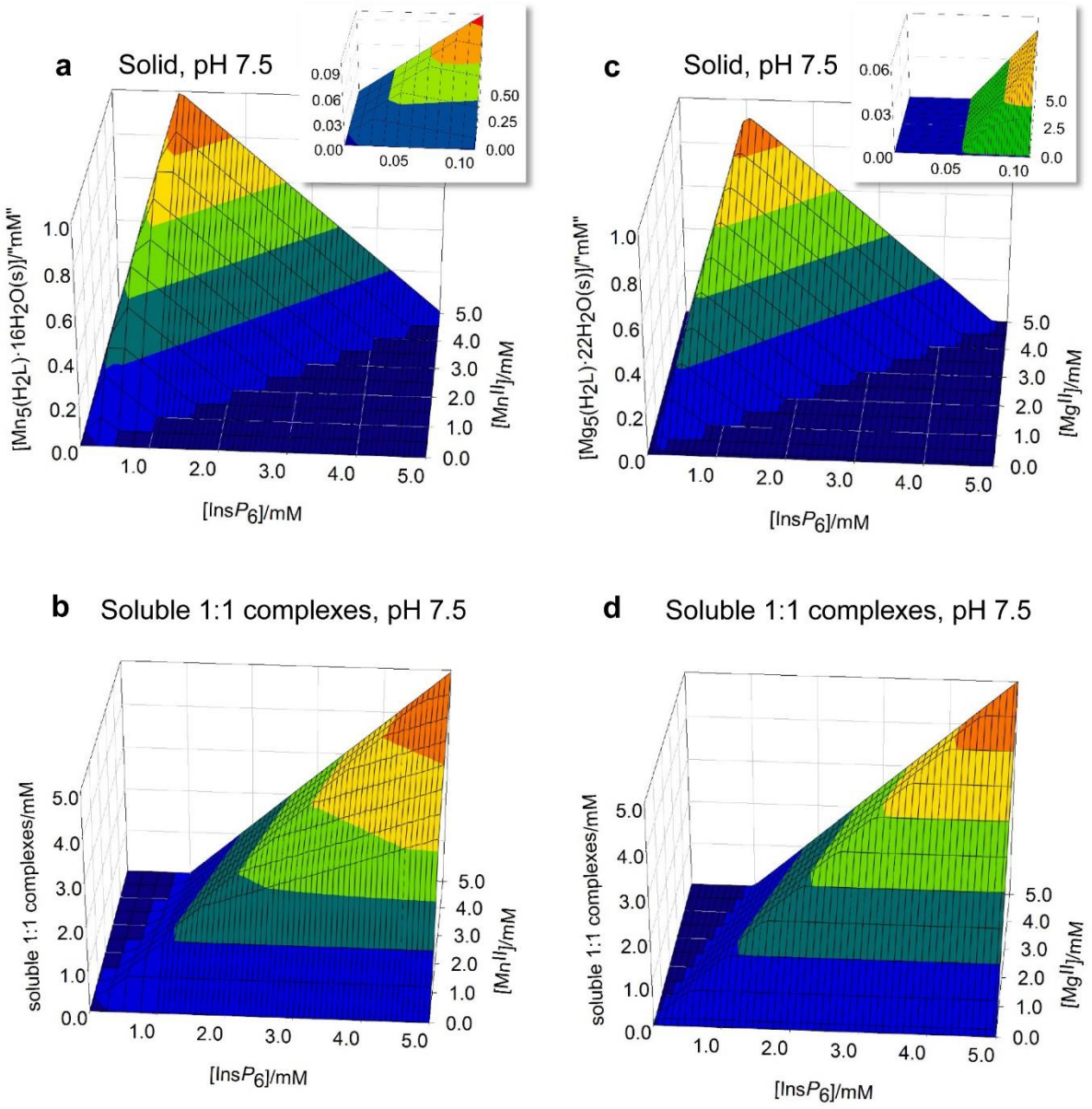

Figure 4. Behavior of InsP_6 in the presence of manganese(II). The graphs show the predicted abundances of solid manganese phytate (a) and of the sum of the different soluble 1:1 Mn:InsP_6 complexes (b), plotted against total concentrations of InsP_6 and Mn(II). In c and d, the same information is shown for Mg-phytate system[13]. Predictions are drawn for pH 7.5, in 0.15 M $NaClO_4$ and 37.0 °C. The insets in a) and c) show a "zoom-in" of the low InsP_6 concentration range.

the PO-H scissoring modes. At lower wavenumbers, numerous normal modes are detected, although a detailed assignment is not straightforward. The stretching of P–OC bonds and the O–P–O bending vibrations of phytate are observable at 586 and 511 cm^{-1}, respectively, while a very intense peak at 775 cm^{-1} can be attributed to the ρ(C–H) modes of terpy, which was also found for other terpy complexes.[29]

Crystal structure of 2

Crystals of $(H_2terpy)_2[Mn(H_6L)(terpy)(H_2O)]\cdot 17H_2O$ are constituted by 1D coordination polymers developing along [100] direction (Figure 5). Each Mn(II) cation is hexacoordinated in a strongly distorted octahedral environment by the three nitrogen atoms of a terpyridine molecule, a water molecule and two oxygen atoms belonging to two symmetry related phytate anions (see Table 2). The equatorial plane is defined by the terpyridine nitrogen atoms and the coordinated water molecule, while the phytate oxygen atoms occupy the apical positions. The metal atom is 0.039(3) Å displaced from the equatorial plane. The metal-metal distance between contiguous Mn atoms is 10.3486(7) Å. A similar distance (10.2 Å) separates two consecutive coordinated terpyridine groups. This distance is divided into three almost equal sections by two intercalated terpyridine molecules (interplanar π-π contact distances *ca* 3.4 Å).

As the acidic hydrogens were not clearly found in the ΔF map, different formulas, differing for the location of acidic protons in the solid complex, could be possible. On the basis of phytate

Accepted Manuscript

This article is protected by copyright. All rights reserved.

Table 2. Selected bond distances (Å) and angles (deg) for the metal coordination environment. (e.s.d. in parentheses).

Mn01-O52 2.12(1)	Mn01-N2C 2.29(2)	Mn01-OW1 2.14(1)	
Mn01-O63' 2.13(1)	Mn01-N1C 2.28(2)	Mn01-N3C 2.29(2)	
N1C-Mn01-N2C 70.8(6)	N2C-Mn01-N3C 70.4(6)	N3C-Mn01-O52 100.8(5)	O52-Mn01-O63' 159.6(5)
N1C-Mn01-N3C 141.20(6)	N2C-Mn01-O52 98.3(5)	N3C-Mn01-O63' 95.4(5)	O52-Mn01-OW1 80.7(5)
N1C-Mn01-O52 85.8(5)	N2C-Mn01-O63' 98.7(5)	N3C-Mn01-OW1 93.7(6)	O63'-Mn01-OW1 86.0(5)
N1C-Mn01-O63' 89.3(5)	N2C-Mn01-OW1 163.7(6)		
N1C-Mn01-OW1 125.1(5)			

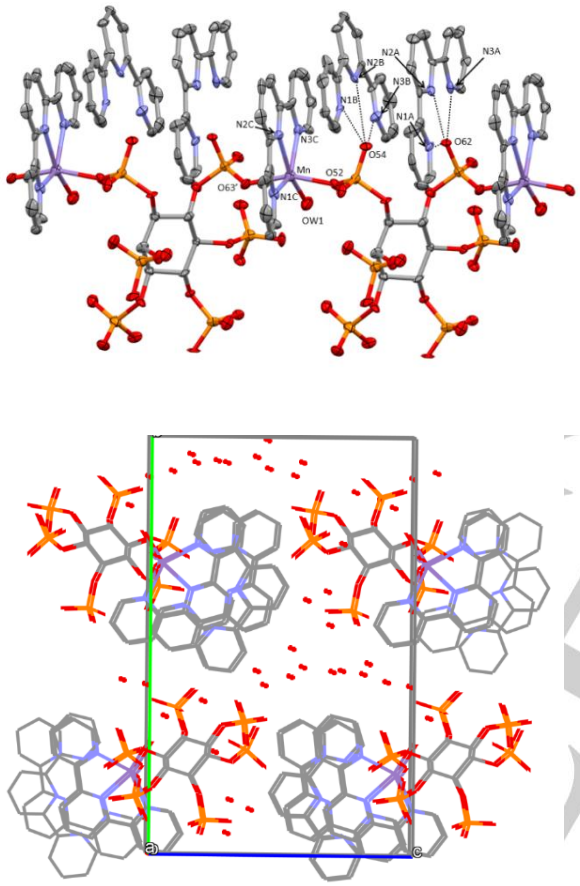

Figure 5. Crystal structure of $(H_2terpy)_2[Mn(H_6L)(terpy)(H_2O)]\cdot 17H_2O$ (**2**). Up: 1D coordination polymers developing along [100] direction. Thermal ellipsoids are plotted at the 40% probability level. Down: view of the crystal packing (hydrogen atoms are omitted for clarity). Color code: C (grey), H (white), O (red), N (blue), P (orange), Mn (violet).

and terpy protonation constants and the experimental conditions adopted for the synthesis of the complex, $(H_2terpy)_2[Mn(H_6L)(terpy)(H_2O)]\cdot 17H_2O$ would reflect the most reasonable distribution of acidic protons among the basic sites of the complex (see below). In any case, very short H-bond contacts are established between the two intercalated terpyridine molecules and the same phytate anion (N1A···O62 2.67(2), N2A···O62 2.90(2), N3A···O62 2.58(2), N1B···O54 2.67(2), N2B···O54 3.00(2), N3B···O54 2.65 (2) Å, Figure 5).

Table 3. Logarithms of the equilibrium constants for the reactions $p\ Mn^{2+} + q\ terpy + r\ L^{12-} + s\ H^+ \rightarrow Mn_p(terpy)_qL_rH_s$, in 0.15 M NMe_4Cl at 37.0 °C.

System	*pqrs*	log β_{pqrs} [a]	σ[a]	log β_{pqrs} [b]
Mn(II)-terpy	1100	5.59(2)	0.79	8.84(6)
	1200	10.04(2)		15.27(6)
	110–1	-3.33(4)		
	220–2			4.4(1)
Mn(II)-terpy-InsP_6	1112		0.76	36.34(2)
	1113	44.0(1)		46.15(3)
	1114	52.25(6)		54.88(3)
	1115	58.88(6)		61.56(5)
	1116	64.30(6)		66.94(6)
	1117	67.89(7)		70.17(7)
	1118	70.9(1)		72.35(9)
	1119	73.86(7)		
	11110	76.1(2)		
	2114			59.78(6)
	2211	37.4(1)		
	2212	46.3(2)		
	2213	55.17(7)		59.46(5)
	2214	61.6(2)		66.97(6)
	3214			72.80(5)
	3313			72.51(4)
	4411			67.28(4)
	4412			76.25(8)

[a] This work. σ represents the scaled sum of square differences between predicted and experimental values. Values given in parentheses are the 1σ statistical uncertainties in the last digit of the constant. [b] Values for the analogous systems with Cu(II) reported previously under the same conditions are included for comparison.[20a]

As already observed in the crystal structures containing phytate anions previously reported in the literature,[20, 30] the overall packing is additionally stabilized by a dense H-bond network involving the high number of co-crystallized water molecules (Figure 5).

Chemical speciation of Mn(II)-terpy-InsP_6 system

Table 3 shows the results obtained in the potentiometric studies. The interaction of Mn(II) with terpy was also studied in 0.15 M NMe_4Cl at 37.0 °C as the first step. Results are similar to previously reported values under different experimental conditions.[31] The most relevant species in the Mn(II)-terpy

Accepted Manuscript

This article is protected by copyright. All rights reserved.

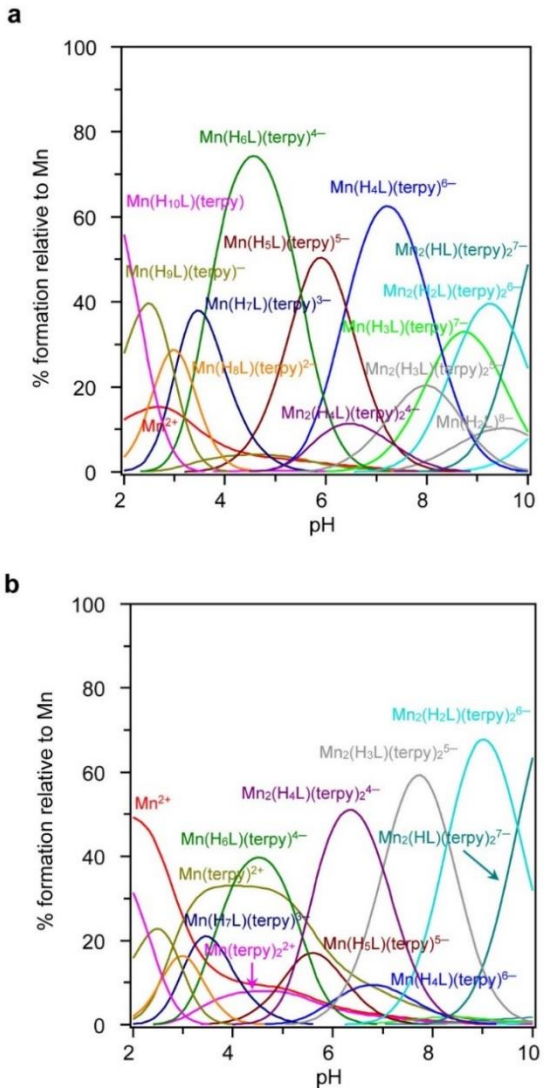

Figure 6. Species distribution diagrams for Mn(II)-terpy-InsP_6 system, in 0.15 M NMe_4Cl at 37.0 °C. a) [Mn(II)] = [InsP_6] = [terpy] = 1 mM. b) [Mn(II)] = [terpy] = 2 mM, [InsP_6] = 1 mM.

system are $[Mn(terpy)]^{2+}$ and $[Mn(terpy)_2]^{2+}$. The fact that the Mn(II) coordination sphere can be partially occupied by the aromatic amine as auxiliary ligand, would promote the formation of a ternary Mn-InsP_6-terpy compound favoring the isolation of a crystalline compound.

In fact, for the systems containing the three components (terpy, InsP_6 and manganese(II)), various protonated species with 1:1:1 molar ratio are among the most important complexes formed in solution (Figure 6a). Besides, some polynuclear species (manganese:terpy:InsP_6) 2:2:1, 3:3:1 or 4:4:1 are also detected. As expected, these polynuclear species become predominant for phytate defect conditions (Figure 6b). The stoichiometries of the detected species are very similar to the results obtained for Cu(II):terpy:InsP_6 system (last column in Table 3)[20a], showing lower stability constant values in the case of Mn(II), reflecting the electrostatic character of the interaction.

The species $[Mn(H_6L)(terpy)]^{4-}$ found in the solid complex **2** was also detected in solution (Figure 6a). It forms above pH 2 and predominates at *ca*. pH 4 for 1:1:1 manganese(II):terpy:InsP_6 molar ratio. Notwithstanding, compound **2** was only isolated if the pH was adjusted to 2.6, probably due to the necessary protonation of the amine to generate the solid compound (Figure S5). Although this is a plausible explanation, we cannot exclude that a different assembly process takes place starting from other protonated ternary species.

In order to furnish a picture of a possible assembling mechanism different $[Mn(H_6L)(terpy)]^{4-}$ microspecies were DFT optimized, starting from the structural parameters obtained for compound **2**. This is shown in Figure 7. In line with the magnetic measurements (see experimental), manganese(II) high-spin state gave place to more stable adducts. Among the two tested $[Mn(H_6L)(terpy)]^{4-}$ microspecies, the most stable one was that involving metal coordination *via* the phytate phosphate group in C6. This species can be thought as the most contributing in solution that could in turn give place to the assembly of compound **2**.

Conclusions

The interaction of InsP_6 with inorganic and organic cations has been recognized to be of utmost importance to understand the function of this molecule in biological environments. In this work we expanded the study to the system Mn(II)-phytate. Soluble species with 1:1 molar ratio are predominant if excess of phytate is present in solution. All the species are anionic and differ in the protonation degree of phytate, which becomes lower as pH increases. A solid phase appears as the amount of Mn(II) is increased, especially at high pH values. This solid was characterized as $Mn_5(H_2L)\cdot16H_2O$ (**1**) and its solubility was determined as $\log K_{s0} = -39.9(9)$ at 0.15 M $NaClO_4$ and 37.0 °C. This data is essential for a complete thermodynamic picture of the Mn(II)-phytate system over a wide pH range including those found in many biological media.

The coordination mode of phytate in the presence of Mn(II) was analyzed for the ternary system Mn(II)-phytate-terpy. The complex $(H_2terpy)_2[Mn(H_6L)(terpy)(H_2O)]\cdot17H_2O$ (**2**) was isolated and fully characterized by X-ray diffraction, being the first reported structure containing Mn(II) and phytate. The formation of polymeric chains in the structure was also observed in the case of $[Cu_2(H_8L)(terpy)_2]\cdot7.5H_2O$,[20a] but the coordination mode of phytate is not equivalent. The most stable conformation of InsP_6 in acidic solution shows 1 axial and 5 equatorial phosphate groups (Figure 1). The single axial phosphate group is responsible for the formation of the chain in $[Cu_2(H_8L)(terpy)_2]\cdot7.5H_2O$, joining [Cu(terpy)] units through a μ_2-$\eta^1\eta^1$ bridge. In compound **2**, the axial phosphate group remains free and does not participate in the coordination. The connection between [Mn(terpy)] units is sustained through contiguous equatorial phosphate groups acting as monodentate ligands. This structure is a novel example of the multifaceted coordination ability of InsP_6.

Accepted Manuscript

This article is protected by copyright. All rights reserved.

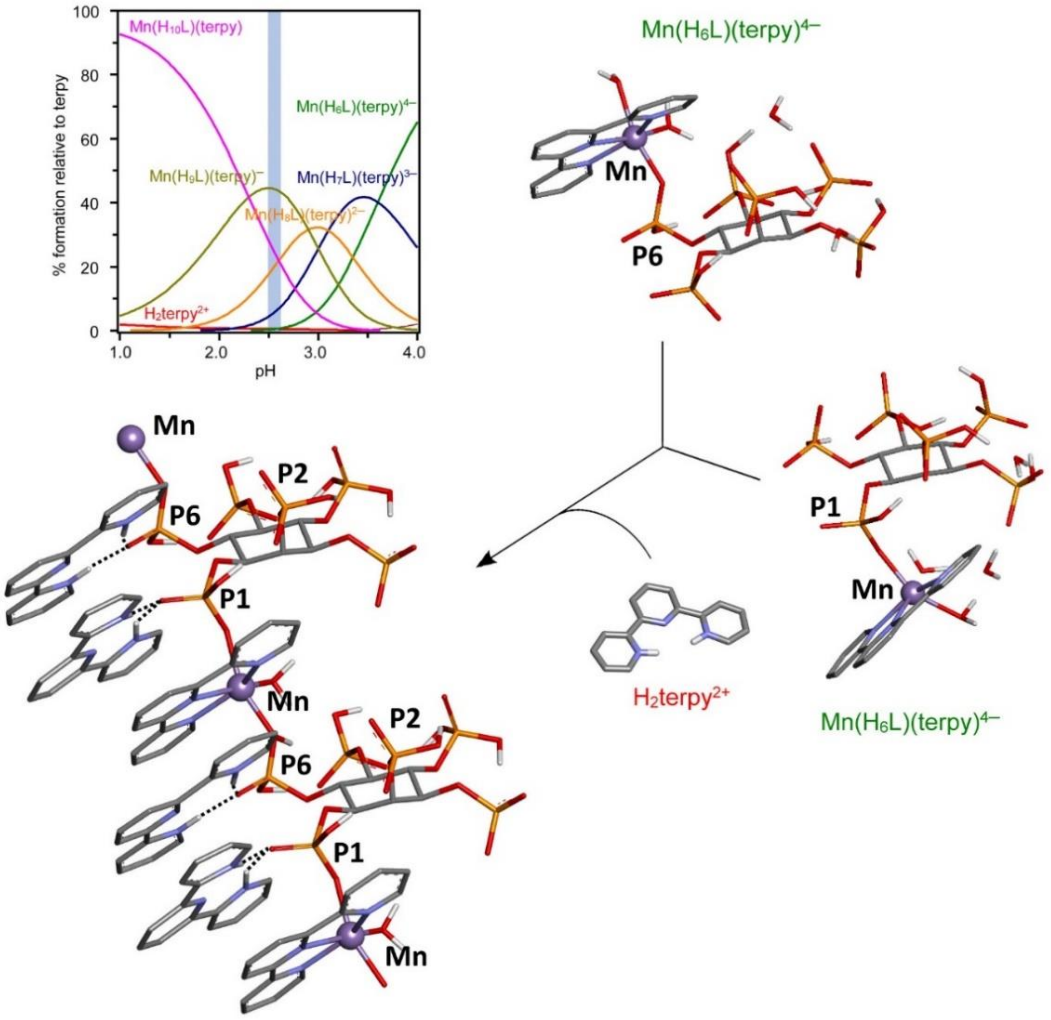

Figure 7. A possible mechanism for self-assembling of Mn(II)-phytate-terpy soluble species to form $(H_2terpy)_2[Mn(H_6L)(terpy)]$. All involved species are formed in solution under the experimental conditions adopted to synthesize the complex according to the distribution diagram reported in the inset ([terpy] = [InsP_6] = [Mn(II)] = 15 mM; minor species were omitted for clarity). Structures of $Mn(H_6L)(terpy)^{4-}$ isomers are geometry optimized at UB3LYP/LANL2DZ SMD level of theory. Color code: C (grey), H (white), O (red), N (blue), P (orange), Cu (pink).

Experimental

All chemicals were purchased from commercial sources and used without further purification. $Mn(ClO_4)_2{\cdot}6H_2O$ (Alfa Aesar, >99%) was used as metal source for the synthesis; $MnCl_2{\cdot}4H_2O$ (Sigma, >99%) was used for potentiometric measurements. 2,2´:6´2´´-terpyridine (98%) was supplied from Sigma-Aldrich. The dipotassium salt of InsP_6, $K_2H_{10}L{\cdot}2.5\ H_2O$, was purchased from Sigma-Aldrich and its purity was rechecked by elemental and thermogravimetric analyses. Methanol and ethanol (99%) were obtained from Dorwill. All aqueous solutions were prepared with ultrapure water obtained from a Millipore-MilliQ plus system (up to 18 MΩ cm^{-1}) and used immediately after preparation. The ionic strength was adjusted to 0.15 M with NMe_4Cl or $NaClO_4$ (Fluka). The standard HCl solutions were prepared by diluting Merck standard ampoules. The titrant solution (0.1 M NMe_4OH in 0.15 M NMe_4Cl) was prepared by dissolving $NMe_4OH{\cdot}5H_2O$ (Fluka), and was standardized with potassium biphthalate. Mn(II) solutions were standardized according to standard techniques.[32]

Synthesis

$Mn_5(H_2L){\cdot}16H_2O$ (1)

A 0.01 M aqueous solution of InsP_6 was prepared and its pH adjusted to 10 by the addition of 1 M LiOH. To 30 mL (0.3 mmol) of this solution, 0.54 g $Mn(ClO_4)_2{\cdot}6H_2O$ (1.5 mmol) dissolved in the minimum amount of water was added. A beige solid (344 mg, 95%) immediately formed, which was separated by centrifugation, thoroughly washed with water (3 x 10 mL), then with ethanol (2 x 10 mL) and air-dried: IR (KBr): ν=3400, 1655, 1090, 991, 546 cm^{-1}; elemental analysis calcd (%) for $Mn_5C_6H_{40}O_{40}P_6$ (1212.89): C 5.9, H 3.3, Mn 22.7; found: C 5.9, H 3.1, Mn 22.9; thermal analysis agreed with the proposed formula: 24.7% weight loss corresponding to the elimination of water, compared with a calculated value of 23.8%.

$(H_2terpy)_2[Mn(H_6L)(terpy)(H_2O)]{\cdot}15H_2O$ (2)

Accepted Manuscript

This article is protected by copyright. All rights reserved.

27 mg of **1** (0.022 mmol) was dissolved in 0.4 mL aqueous solution of $K_2H_{10}L{\cdot}2.5\ H_2O$ (69 mg, 0.088 mmol) and 5 mL of water was added. Finally, 2 mL of a solution of terpy (26 mg, 0.11 mmol) in methanol was slowly added with stirring (pH *ca.* 2.6). Yellow crystals of **2** (21 mg, 34%) were obtained by slow solvent evaporation at room temperature, and were collected by filtration and air-dried: *v*=3426, 1618, 1450, 1175, 1067, 993, 775, 511 cm^{-1}; elemental analysis calcd (%) for $C_{51}H_{81}N_9O_{40}P_6Mn_1$ (1701.02): N 7.4, C 36.0, H 4.8; found: N 7.3, C 36.1, H 4.8; thermal analysis agreed with the proposed formula: 16.9% weight loss corresponding to the elimination of water, compared with a calculated value of 17.0%. μ_{obs} = 5.91 B.M. per Mn atom. Several crystals, of X-ray diffraction quality, taken from different batches of compound **2,** gave crystal structures corresponding to the formula $(H_2terpy)_2[Mn(H_6L)(terpy)(H_2O)]{\cdot}17H_2O$. Throughout this work, **2** was used to indicate both $(H_2terpy)_2[Mn(H_6L)(terpy)(H_2O)]{\cdot}15H_2O$ and $(H_2terpy)_2[Mn(H_6L)(terpy)(H_2O)]{\cdot}17H_2O$.

Infrared spectroscopy, elemental analysis, thermal analysis and magnetic measurements

Infrared spectroscopy was carried out on a Shimadzu FT-IR spectrophotometer, with samples present as 1% KBr pellets. The assignation of the most important infrared bands was carried out according to previously reported works on related systems.[20-21, 28-29] Elemental analysis (N, C, H) was performed on a Thermo Scientific FLASH 2000 CHNS/O instrument. Thermal analysis was performed on a Shimadzu TGA-50 instrument with a TA 50 I interface, using a platinum cell and nitrogen atmosphere. Experimental conditions were 0.5 °C min^{-1} temperature ramp rate and 50 mL min^{-1} nitrogen flow rate. Magnetic measurements at r.t. were performed on a Quantum Design MPMS SQUID magnetometer. Diamagnetic corrections were estimated using Pascal constants.

Solubility determinations

Solubility measurements of compound **1** were carried out at constant ionic strength *I* = 0.15 M $NaClO_4$ and 37.0 °C, following the procedure applied earlier for alkaline-earth phytates.[13, 21] Approximately 100 mg of compound **1** was suspended in 15 mL 0.15 M aqueous $NaClO_4$. Known amounts of HCl were added, so as to reach equilibrium points corresponding to measurable amounts of manganese in solution. Each mixture was kept in a glass jacketed cell at 37.0 °C under continuous stirring until measured pH was constant (*ca.* one week). After the equilibrium was reached, excess solid was filtered out (0.20 µm pore size Minisart® Sartorius disk filter), and manganese concentration was determined in the supernatant.[32] Starting from these Mn concentration values, and assuming a 5:1:2 stoichiometry (Mn(II):InsP_6:H^+), total amounts of H^+ and InsP_6 were calculated. This information was used as an input in the HySS software[24] to determine the equilibrium concentrations of free Mn^{2+} and H_2L^{10-} species, which define the K_{s0}. In this calculation, the thermodynamic data of the complete set of equilibria involved[12] were taken into account.

X-ray diffraction analysis

A yellow crystal of $(H_2terpy)_2[Mn(H_6L)(terpy)(H_2O)]{\cdot}17H_2O$ (**2**) was used for X-ray diffraction analysis. The integrated intensities were corrected for Lorentz and polarization effects and an empirical absorption correction was applied.[33] The structures were solved by direct methods (SHELXS-86).[34] Refinements were performed by means of full-matrix least-squares using SHELXL Version 2014/7 program.[35] All the non-hydrogen atoms were anisotropically refined. Terpyridine hydrogen atoms were introduced in calculated position and their coordinates were refined according to the linked atoms. We were not able to clearly localize hydrogen atoms belonging to phytate, protonated terpyridine units and cocrystallized water molecules. Thus these hydrogens were not introduced in the calculation. Details of data collection and refinement are summarized in Table 4. The CCDC number for **2**, 1523045, contains the supplementary crystallographic data for this paper. These data can be obtained free of charge from The Cambridge Crystallographic Data Centre via www.ccdc.cam.ac.uk/data_request/cif.

Table 4. Crystal data and structure refinement for $(H_2terpy)_2[Mn(H_6L)(terpy)]{\cdot}17H_2O$ (**2**).

Empirical formula	$C_{51}H_{85}MnN_9O_{42}P_6$
Formula weight	1737.03
Temperature (K)	150
crystal system	monoclinic
space group	*P2₁*
a (Å)	10.3486(7)
b (Å)	23.861(1)
c (Å)	15.315(1)
β (°)	101.732(8)
Volume (Å^3)	3702.7(4)
Z	2
ρ_{calcd} (g cm^{-3})	1.558
Independent reflections / R(int)	9499 / 0.1374
μ (mm^{-1}, Mo-Kα)	0.414
R indices [I>2σ(I)][a]	R1 = 0.0478
	wR2 = 0.0964
R indices (all data)[a]	R1 = 0.0681
	wR2 = 0.1049

[a] R1 = Σ || Fo| - |Fc|| / Σ |Fo|. wR2 = [Σ w(Fo^2 - Fc^2) ^{2} / Σ wFo^4]½.

Potentiometric measurements

The chemical behavior of terpy-Mn(II) system in the presence and absence of InsP_6 was analyzed through potentiometric titrations in 0.15 M NMe_4Cl at 37.0 °C, according to our previous works.[20] Experimental details of titrations are listed in Table S1. The equilibrium constants for phytate and terpy protonation, Mn(II)-InsP_6 complexes formation and phytate-terpy interaction measured under the same conditions were taken from our previous reports.[12, 14, 20a]

Potentiometric data were analyzed by using the HYPERQUAD program.[36] The fit of the values predicted by the model to the experimental data was estimated on the basis of the σ parameter, corresponding to the scaled sum of square differences between predicted and experimental values. Many other possible stoichiometries were tried for each system, and final models were selected on the basis of the σ parameter, the model confidence level estimator, chi-square, and the internal consistency of data reflected in standard deviations of the formation constants.[36] Species distribution diagrams were produced by using the HySS program.[24]

Computational calculations

All the calculations were run by means of the methods described hereinafter as implemented in Gaussian 09.[37] The interaction with the bulk of the solvent was modeled through an IEFPCM method, with radii and non-electrostatic terms from Truhlar and coworkers' SMD solvation model.[38] The final structures obtained were all minima in the potential energy surface, being the nature of the stationary points verified through

Accepted Manuscript

This article is protected by copyright. All rights reserved.

vibrational analysis. The outputs were rendered with Discovery Studio Visualizer software.[39]

In order to make a detailed assignment of the infrared spectra of the dipotassium salt, the vibrational normal modes of the totally protonated phytate anion were calculated at RHF/3-21+G* level of theory. The modelling of the $H_{10}L^{2-}$ anion present in the dipotassium salt was not possible, since there is no data on its protonation pattern. The optimized geometry of $H_{12}L$ was taken from our previously reported data.[40] For the molecular modeling approach to the 1:1:1 Mn(II):InsP_6:terpy complexes, unrestricted Density Functional Theory (DFT) geometry optimization runs were carried out, using the B3LYP functional and the effective core potential LANL2DZ basis set.[41] The initial geometries were built using the information given by the crystal structure of **2**, and the phytate protonation pattern was fixed according to the relative position of the ionisable groups. Water molecules were placed to complete the metal coordination sphere. Manganese(II) high- and low-spin states were considered and the most stable geometries were selected.

Acknowledgements

The authors are grateful to CSIC (Programa de Apoyo a Grupos de Investigación, Uruguay) for financial support. Financial support from the Italian MIUR (project 2015MP34H3) is gratefully acknowledged.

Keywords: chemical speciation • manganese • phytate • solubility product • X-ray diffraction

[1] F. A. Cotton, G. Wilkinson, *Advanced Inorganic Chemistry*, Wiley, New York, **1999**.

[2] D. W. Christianson, *Progress in Biophysics and Molecular Biology* **1997**, *67*, 217-252.

[3] J. J. R. Fraústo da Silva, R. J. P. Williams, *The Biological Chemistry of the Elements: The Inorganic Chemistry of Life*, second ed., OUP Oxford, New York, **2001**.

[4] E. C. Theil, K. N. Raymond, in *Bioinorganic Chemistry* (Eds.: I. Bertini, H. D. Gray, S. J. Lippard, J. S. Valentine), University Science Books, Mill Valley, CA, **1994**, pp. 1-35.

[5] D. E. Ash, V. L. Schramm, *Journal of Biological Chemistry* **1982**, *257*, 9261-9264.

[6] H. Sigel, *Metal Ions in Biological Systems: Volume 37: Manganese and Its Role in Biological Processes*, Taylor & Francis, **2000**.

[7] F. Galiazzo, J. Z. Pedersen, P. Civitareale, A. Schiesser, G. Rotilio, *Biology of Metals* **1989**, *2*, 6-10.

[8] a) A. R. Reddi, L. T. Jensen, A. Naranuntarat, L. Rosenfeld, E. Leung, R. Shah, V. C. Culotta, *Free Radical Biology and Medicine* **2009**, *46*, 154-162; b) M. Al-Maghrebi, I. Fridovich, L. Benov, *Archives of Biochemistry and Biophysics* **2002**, *402*, 104-109; c) M. J. Daly, *Nat Rev Micro* **2009**, *7*, 237-245; d) F. S. Archibald, I. Fridovich, *Journal of Bacteriology* **1981**, *145*, 442-451; e) Y. T. Lin, H. Hoang, S. I. Hsieh, N. Rangel, A. L. Foster, J. N. Sampayo, G. J. Lithgow, C. Srinivasan, *Free Radical Biology and Medicine* **2006**, *40*, 1185-1193; f) R. J. Sanchez, C. Srinivasan, W. H. Munroe, M. A. Wallace, J. Martins, T. Y. Kao, K. Le, E. B. Gralla, J. S. Valentine, *JBIC Journal of Biological Inorganic Chemistry* **2005**, *10*, 913-923.

[9] a) A. Benedetto, C. Au, M. Aschner, *Chemical Reviews* **2009**, *109*, 4862-4884; b) C. G. Worley, D. Bombick, J. W. Allen, R. Lee Suber, M. Aschner, *NeuroToxicology* **2002**, *23*, 159-164.

[10] R. L. McNaughton, A. R. Reddi, M. H. S. Clement, A. Sharma, K. Barnese, L. Rosenfeld, E. B. Gralla, J. S. Valentine, V. C. Culotta, B. M. Hoffman, *Proceedings of the National Academy of Sciences* **2010**, *107*, 15335-15339.

[11] M. Bennett, S. M. N. Onnebo, C. Azevedo, A. Saiardi, *Cellular and Molecular Life Sciences* **2006**, *63*, 552-564.

[12] J. Torres, S. Domínguez, M. F. Cerdá, G. Obal, A. Mederos, R. F. Irvine, A. Díaz, C. Kremer, *Journal of Inorganic Biochemistry* **2005**, *99*, 828-840.

[13] N. Veiga, J. Torres, S. Domínguez, A. Mederos, R. F. Irvine, A. Díaz, C. Kremer, *Journal of Inorganic Biochemistry* **2006**, *100*, 1800-1810.

[14] N. Veiga, I. Macho, K. Gómez, G. González, C. Kremer, J. Torres, *Journal of Molecular Structure* **2015**, *1098*, 55-65.

[15] R. Hell, R. R. Mendel, *Cell Biology of Metals and Nutrients*, Springer Berlin Heidelberg, **2010**.

[16] S. K. Sathe, N. R. Reddy, *Food Phytates*, CRC Press, **2002**.

[17] a) L. Davidsson, A. Almgren, M. A. Juillerat, R. F. Hurrell, *American Journal of Clinical Nutrition* **1995**, *62*, 984-987; b) B. Lonnerdal, *International Journal of Food Science and Technology* **2002**, *37*, 749-758.

[18] C. Bretti, R. M. Cigala, C. De Stefano, G. Lando, S. Sammartano, *Journal of Chemical & Engineering Data* **2012**, *57*, 2838-2847.

[19] U. P. Rodrigues-Filho, J. Vaz, M. P. Felicissimo, M. Scarpellini, D. R. Cardoso, R. C. J. Vinhas, R. Landers, J. F. Schneider, B. R. McGarvey, M. L. Andersen, L. H. Skibsted, *Journal of Inorganic Biochemistry* **2005**, *99*, 1973-1982.

[20] a) N. Veiga, J. Torres, C. Bazzicalupi, A. Bianchi, C. Kremer, *Chemical Communications* **2014**, *50*, 14971-14974; b) D. Quiñone, N. Veiga, J. Torres, J. Castiglioni, C. Bazzicalupi, A. Bianchi, C. Kremer, *Dalton Trans* **2016**, *45*, 12156-12166.

[21] J. Torres, N. Veiga, J. S. Gancheff, S. Domínguez, A. Mederos, M. Sundberg, A. Sánchez, J. Castiglioni, A. Díaz, C. Kremer, *Journal of Molecular Structure* **2008**, *874*, 77-88.

[22] a) W. J. Evans, M. A. Marini, C. J. Martin, *Journal of Inorganic Biochemistry* **1983**, *19*, 129-132; b) W. J. Evans, C. J. Martin, *Journal of Inorganic Biochemistry* **1988**, *32*, 259-268; c) W. J. Evans, C. J. Martin, *Journal of Inorganic Biochemistry* **1988**, *34*, 11-18; d) W. J. Evans, C. J. Martin, *Journal of Inorganic Biochemistry* **1992**, *45*, 105-113; e) A. Bebot-Brigaud, G. Dange, N. Fauconnier, C. Gérard, *Journal of Inorganic Biochemistry* **1999**, *75*, 71-78; f) C. J. Martin, W. J. Evans, *Journal of Inorganic Biochemistry* **1986**, *27*, 17-30; g) F. Grynspan, M. Cheryan, *Journal of the American Oil Chemists' Society* **1983**, *60*, 1761-1764; h) W. J. Evans, A. G. Pierce, *Journal of the American Oil Chemists' Society* **1981**, *58*, 850-851.

[23] J. Xu, D. F. R. Gilson, I. S. Butler, *Spectrochimica Acta Part A* **1998**, *54*, 1869-1878.

[24] L. Alderighi, P. Gans, A. Ienco, D. Peters, A. Sabatini, A. Vacca, *Coordination Chemistry Reviews* **1999**, *184*, 311-318.

[25] D. Lien-Vien, N. B. Colthup, W. G. Fateley, J. G. Graselli, *The Handbook of Infrared and Raman Characteristics Frequencies of Organic Molecules*, Academic Press, Inc., California, USA, **1991**.

[26] F. Barlt, H. Urjasz, B. Brzezinski, *Journal of Molecular Structure* **1998**, *441*, 77-82.

[27] S. Youngme, P. Phuengphai, N. Chaichit, C. Pakawatchai, G. A. van Alvada, O. Roubeau, J. Reedijk, *Inorganica Chimica Acta* **2004**, *357*, 3603-3612.

[28] K. Nakamoto, *Infrared and Raman Spectra of Inorganic and Coordination Compounds, Part B, Applications in Coordination, Organometallic, and Bioinorganic Chemistry*, 6th ed., John Wiley & Sons, Inc., New York, **2009**.

[29] N. Alvarez, N. Veiga, S. Iglesias, M. H. Torre, G. Facchin, *Polyhedron* **2014**, *68*, 295-302.

[30] G. E. Blank, J. Pletcher, M. Sax, *Acta Crystallographica* **1975**, *B31*, 2584-2592.

[31] a) M. Ignaczak, G. Andrijewski, *Zhurnal Neorganicheskoi Khimii* **1992**, *37*; b) D. J. Benton, P. Moore, *Journal of the Chemical Society, Dalton*

Accepted Manuscript

This article is protected by copyright. All rights reserved.

Transactions **1973**, 399-404; c) R. H. Holyer, C. D. Hubbard, S. F. A. Kettle, R. G. Wilkins, *Inorganic Chemistry* **1966**, *5*, 622-625.
[32] G. Schwarzenwach, H. Flaschka, *Complexometric Titrations*, 2nd ed., Methuen, London, **1969**.
[33] Agilent Technologies, **2015**.
[34] G. Sheldrick, *Acta Crystallographica Section A* **1990**, *46*, 467-473.
[35] G. Sheldrick, *Acta Crystallographica Section C* **2015**, *71*, 3-8.
[36] P. Gans, A. Sabatini, A. Vacca, *Talanta* **1996**, *43*, 1739-1753.
[37] M. J. Frisch, G. W. Trucks, H. B. Schlegel, G. E. Scuseria, M. A. Robb, J. R. Cheeseman, G. Scalmani, V. Barone, B. Mennucci, G. A. Petersson, H. Nakatsuji, M. Caricato, X. Li, H. P. Hratchian, A. F. Izmaylov, J. Bloino, G. Zheng, J. L. Sonnenberg, M. Hada, M. Ehara, K. Toyota, R. Fukuda, J. Hasegawa, M. Ishida, T. Nakajima, Y. Honda, O. Kitao, H. Nakai, T. Vreven, J. Montgomery, J. E. Peralta, F. Ogliaro, M. J. Bearpark, J. Heyd, E. N. Brothers, K. N. Kudin, V. N. Staroverov, R. Kobayashi, J. Normand, K. Raghavachari, A. P. Rendell, J. C. Burant, S. S. Iyengar, J. Tomasi, M. Cossi, N. Rega, N. J. Millam, M. Klene, J. E. Knox, J. B. Cross, V. Bakken, C. Adamo, J. Jaramillo, R. Gomperts, R. E. Stratmann, O. Yazyev, A. J. Austin, R. Cammi, C. Pomelli, J. W. Ochterski, R. L. Martin, K. Morokuma, V. G. Zakrzewski, G. A. Voth, P. Salvador, J. J. Dannenberg, S. Dapprich, A. D. Daniels, Ö. Farkas, J. B. Foresman, J. V. Ortiz, J. Cioslowski, D. J. Fox, Gaussian, Inc., Wallingford, CT, USA, **2009**.
[38] A. V. Marenich, C. J. Cramer, D. G. Truhlar, *The Journal of Physical Chemistry B* **2009**, *113*, 6378-6396.
[39] 2.5.5.9350 ed., Accelrys Software Inc., **2009**.
[40] N. Veiga, J. Torres, I. Macho, K. Gomez, G. Gonzalez, C. Kremer, *Dalton Transactions* **2014**, *43*, 16238-16251.
[41] P. J. Hay, W. R. Wadt, *Journal of Chemical Physics* **1985**, *82*, 299-310.

WILEY-VCH
Accepted Manuscript

This article is protected by copyright. All rights reserved.

FULL PAPER

We present the chemical, thermodynamic and structural characterization of phytate-Mn(II) species in a contribution to study the interaction of this molecule with cations. The polynuclear complexes $[Mn_5(H_2L)]$ and $(H_2terpy)_2[Mn(H_6L)(terpy)(H_2O)]$ (terpy = terpyridine) were prepared and characterized by different techniques.

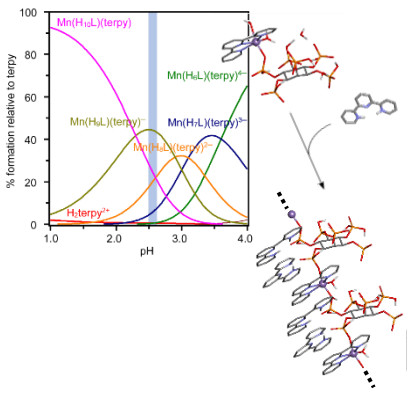

Delfina Quiñone, Nicolás Veiga, Julia Torres, Carla Bazzicalupi, Antonio Bianchi and Carlos Kremer**

Page No. – Page No.

Self-assembly of Mn(II)-phytate coordination polymers: synthesis, crystal structure and physicochemical properties

WILEY-VCH Accepted Manuscript

This article is protected by copyright. All rights reserved.